**Supporting Information for**

# Sonoporation at Small and Large Length Scales. Effect of Cavitation Bubble Collapse on Membranes

Haohao Fu,[†,⊥] Jeffrey Comer,[‡,¶,⊥] Wensheng Cai,[†] and Christophe Chipot[*,‡,§,∥]

*Collaborative Innovation Center of Chemical Science and Engineering (Tianjin), and Research Center for Analytical Sciences, College of Chemistry, Nankai University, Tianjin 300071, China, Laboratoire International Associé Centre National de la Recherche Scientifique et University of Illinois at Urbana-Champaign, Unité Mixte de Recherche n° 7565, Université de Lorraine, B.P. 70239, 54506 Vandœuvre-lès-Nancy cedex, France, Nanotechnology Innovation Center of Kansas State, Institute of Computational Comparative Medicine, Department of Anatomy and Physiology, Kansas State University, P–213 Mosier Hall, Manhattan, Kansas 66506, USA, Theoretical and Computational Biophysics Group, Beckman Institute for Advanced Science and Technology, University of Illinois at Urbana-Champaign, 405 North Mathews, Urbana, Illinois 61801, USA, and Department of Physics, University of Illinois at Urbana-Champaign, 1110 West Green Street, Urbana, Illinois 61801, USA*

E-mail: chipot@ks.uiuc.edu

[*]To whom correspondence should be addressed
[†]Nankai University
[‡]Laboratoire International Associé CNRS/UIUC
[¶]Kansas State University
[§]Theoretical and Computational Biophysics Group
[∥]Department of Physics, UIUC
[⊥]Contributed equally to this work

# Methods

## Design of the simulations

Because bubble collapse is manifestly a nonequilibrium process, the simulation protocols must be carefully considered and may differ from those ordinarily employed in equilibrium simulations, in particular those of bimolecular objects. Here, we describe the setup of our molecular assemblies, the measurement of the impulse delivered to the membrane, and how the temperature and pressure are handled.

Computational feasibility dictates that we can only simulate a small patch of a model membrane enclosed in a nanoscale box with water above and below it. As is often done in molecular dynamics simulations, we construct the system to be substantially bigger than the object of interest — in this case, the bubble, and assume that the effects of interest are local and robust enough that this nanoscale molecular assembly mimics a much larger, meso– , possibly macroscale system utilized in experiments. The size of the nanoscale molecular assembly poses some conceptual difficulties when simulating phenomena like bubble collapse, which involve supersonic flows and transmission of sound waves, due to the high speed of sound in water — typically on the order of $\sim$1500 nm/ns. The size of the object at hand also limits the types of membrane disturbances that can be observed, in particular bending with wavelengths larger than the system size are not possible. Furthermore, real cell membranes may have different mechanical properties due to their composition and rigidity, partially enforced by a cytoskeleton. We, however, show here that the quantity that has been highlighted as the most important for enhancing the permeation of drugs, namely the impulse delivered to the membrane, is rather insensitive to the system size when appropriate simulation protocols are followed.

A small patch of lipid bilayer embedded in a larger membrane resists significant displacements owing to the energy necessary to bend neighboring portions of the membrane. To mimic this resistance in a small membrane patch, we restrain the position of its center of

mass, which can be seen as a virtual spring between the latter and a fixed point. This geometric restraint also conveniently allows the force acting on the lipid bilayer to be measured from the distance over which the virtual spring is stretched. Restraining the center of mass of the membrane, rather than each lipid individually, further permits deformation of the membrane to be observed, which would be suppressed otherwise. In typical equilibrium simulations, one employs thermostatting algorithms that virtually couple the system to a thermal bath to maintain the temperature and generate the relevant canonical ensemble distribution. These algorithms can, however, lead to spurious kinetics[1] and may be unsuitable for a rapid, eminently non-equilibrium process such as bubble collapse. For this reason, previous molecular dynamics simulations of bubble collapse omitted the use of a thermostat.[2] In such simulations, linear momentum is in principle conserved (albeit actual conservation is approximate due to numerical errors), except where external forces, such as geometric restraints acting on the membrane, are applied. Yet, coupled with the periodic boundary conditions typically employed to avoid interfaces, the lack of energy and momentum dissipation results in difficulties in measuring the force exerted on the membrane. Half of the disturbance created by the collapsing bubble travels toward the nearby interfacial environment, where its force is registered by causing displacement of the virtual spring restraining the lipid bilayer. The other half of the disturbance travels away from the membrane, but, due to conservation of linear momentum and periodic boundary conditions, it travels undissipated and eventually strikes the opposite side of the membrane, imparting an impulse exactly opposite to the initial impulse. An example of this phenomenon is shown in Figure S1. To remove the spurious effect of the second impulse, we constructed a system featuring two lipid bilayers as shown in Figure S2. A Langevin thermostat[3] with a friction constant of 5 $ps^{-1}$ was applied to the atoms of the upper membrane only, dissipating any disturbance that reaches it.

We began our simulations with a spherical void, the surface of which was positioned about 1.5–2.0 nm from the aqueous interface. An example of the system is shown in Figure S2. To avoid finite size effects, the bubble occupied 8% or less of the total system volume in all cases,

and the distance between periodic images of the bubble surface were greater than two-thirds of the diameter of the bubble. The system was equilibrated for at least 5 ns with the void maintained by means of an external force, while the pressure was maintained at 1 atm. To initiate the collapse, the geometric restraints were removed and, under atmospheric pressure, the bubble spontaneously collapsed.

## Computational details

Each system consisted of water and two bilayers of 1-palmitoyl-2-oleoyl-*sn*-phosphatidylcholine (POPC) lipids, in either an atomistic or a coarse-grained representation. The dimensions and compositions of the systems simulated in this work are detailed in Table S1. All molecular dynamics simulations were performed using NAMD 2.10.[3]

For the atomistic models, interactions between atoms were calculated in compliance with the CHARMM36 force field,[4] modified for united-atom aliphatic chains.[5] The standard CHARMM version of the TIP3P water model was used. Electrostatic interactions were calculated via the particle mesh Ewald algorithm[6] with a mesh spacing of $< 0.12$ nm. As in Comer et al.,[7] van der Waals forces were smoothly truncated at 0.8–0.9 nm, as implemented with the vdwForceSwitching keyword of NAMD. The equations of motion were integrated with time steps of 2 and 4 fs for short– and long-range interactions.[8] The Settle algorithm[9] rigidified the water molecules, and the Rattle algorithm[10] constrained covalent bonds featuring hydrogen atoms to their equilibrium length.

The coarse-grained water and POPC molecules were constructed as specified in the MARTINI force field,[11] in which groups of 3–5 non-hydrogen atoms are treated as single particles, referred to as "beads". The van der Waals and Coulomb forces were smoothly truncated from 0.9 to 1.2 nm, using the standard MARTINI switching function and standard dielectric constant of 15.0. The equations of motion were integrated with a 30 fs time step. The MARTINI reference article[11] describes the use of standard bead masses (72 Da), as well as the alternative of choosing bead masses consistent with the masses of the corresponding

atoms. In this contribution, we show that the second option yields a much better agreement between the atomistic and coarse-grained models.

To form the bubbles, an external force was applied to water molecules with distances from the bubble center, $r$, less than the desired bubble radius, $D/2$, thereby expelling water from the interior of the bubble. In other words, the force is given by $\mathbf{F}_{\text{bub}} = -k_{\text{bub}}(r - D/2)\hat{r}$, for $r < D/2$ and $\mathbf{F}_{\text{bub}} = 0$, otherwise. The different bubbles examined in this work were first equilibrated for $> 5$ ns with the temperature and the pressure maintained at 300 K and 1 atm, respectively. During both equilibration and collapse simulations, a constant pressure of 101.325 kPa was maintained by means of the Langevin piston method,[12] applied independently along the $z$ axis, normal to the membrane interface, and the $xy$–plane. The $z$–axis is defined to be normal to the planes of the two membranes in their initial configuration. The force acting on the bilayer during collapse was determined by harmonically restraining the $z$ component of the center of mass of all phosphorus atoms of the bilayer — with a force constant $k_{\text{mem}} = 20000$ kcal mol$^{-1}$ nm$^{-2}$. Including all atoms of the bilayer in the calculation of the restraint force led to an unacceptable loss of computational efficiency. The phosphorus atoms were, therefore, chosen out of convenience and to reduce the computational effort. The two choices were nearly equivalent, as the center of mass of the phosphorus atoms never deviated from the center of mass of all membrane atoms by more than 0.03 nm. The force exerted on the lipid bilayer was measured to be the negative of the restoring force of the harmonic restraint, i.e., $\mathbf{F}_{\text{mem}} = -\mathbf{F}_{\text{harm}} = k_{\text{mem}}(z - z_0)\hat{z}$, where $z$ and $z_0$ are the current and the initial $z$ coordinates, respectively, of the center of mass of the lower bilayer.

It should be pointed out that the parameters used in our simulations are empirical and widely validated by equilibrium simulations. Given, however, the violence of the process at hand, the reliability of the time step value ought to be further verified. To explore whether the time step affects the dynamics of bubble collapse, two additional simulations, namely an atomistic simulation with a time step of 0.5 fs and a coarse-grained one with a time step of 20 fs, have been performed. The results (see Figure S3) suggest that the all-atom simulations

with a 2 fs time step and the coarse-grained simulations with a 30 fs time step are suitable to characterize the collapse of cavitation nanobubbles.

Because the focus of the present work is to understand the effect of bubble collapse on a lipid membrane, we have chosen the CHARMM36 force field, which has been rigorously developed to reproduce a number of important mechanical properties of lipid membranes. The CHARMM36 lipid model has been parameterized with the rigid TIP3P model of water, standard to the CHARMM force field; we have, therefore, chosen this model for consistency. It is important to note that the rigid TIP3P water model has not been thoroughly tested at the extremes of temperature and pressure commonly measured at the surface of cavitation bubbles shortly before their complete collapse. These extremes are, nevertheless, quite local in space and time, and most of the water in the system, including that near the membrane, remains near physiological conditions.

**Atomistic and MARTINI coarse-grained models — agreement and limitations.** In general, the MARTINI force field has the ability to reflect the basic features of the dynamics of atomistic force fields. For example, in a recent paper, Santo and Berkowitz[13] showed that the relationship between the shock wave velocity and the particle velocity is somewhat different for MARTINI water than for SPC water, or in experiment. Specifically, at high particle velocities (¿ 2.5 km/s), the shock velocity of MARTINI water is about 13% higher than for SPC water or in experiment. Such extreme speeds are only seen for the largest bubbles simulated in this work.

In the present work, the most crucial property, namely the impulse delivered to the membrane, is an additive effect of the movement of water molecules. The atomistic and the MARTINI coarse-grained models can also yield the same impulses on the membrane, provided that the latter models use realistic masses. See Figure S5. However, given the reduced representation of the MARTINI model, coarse-graining approaches may trade computational efficiency for accuracy in some particular cases. For example, because the coarse-grained

MARTINI water particles embrace four individual molecules, it is not possible to observe the permeation of single water molecules through the lipid bilayer.

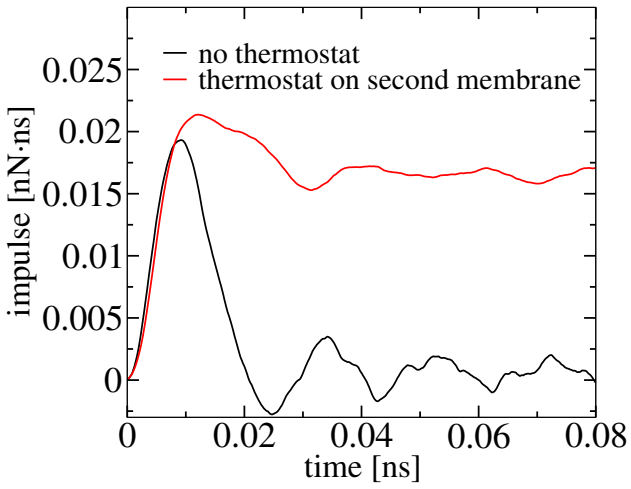


Figure S1: Impulse on a membrane near a collapsing bubble in simulations with periodic boundary conditions. The collapse of the bubble creates disturbances that travel toward and away from the nearby membrane. Without a barrier to dissipate it, the latter eventually crosses most of the system and reaches the membrane, which is an artifact of the periodic boundary conditions that evidently could not occur in experiment. As shown by the black line, the impulse of the half of the disturbance initially moving away from the membrane exactly cancels out that of the half of the disturbance moving toward the membrane. A second membrane to which a thermostatting algorithm is applied can act as a barrier, dissipating the disturbance initially moving away from the membrane, as shown by the red line.

**Table S1: Composition of simulated systems. "A" refers to atomistic models, using the CHARMM36 force field modified for united-atom aliphatic chains, and "CG," to coarse-grained models, using the MARTINI force field.**

| Bubble Diameter (nm) | Model | Number of Atoms/Beads | Number of Water Molecules/Beads | Box Size ($nm^3$) |
|---|---|---|---|---|
| 6 | A | 734,168 | 204,664 | 16.3×16.3×33.4 |
| 8 | A | 734,168 | 204,664 | 16.3×16.3×33.4 |
| 8 | A | 1,045,976 | 308,600 | 16.3×16.3×45.9 |
| 8 | A | 3,003,731 | 841,009 | 32.6×32.6×33.4 |
| 20 | A | 4,197,212 | 1,238,836 | 33.3×33.3×47.0 |
| 15 | CG | 394,157 | 309,709 | 34.4×34.5×49.9 |
| 20 | CG | 394,157 | 309,709 | 34.6×34.8×52.5 |
| 30 | CG | 1,486,585 | 1,296,577 | 53.0×53.2×82.0 |
| 40 | CG | 3,165,977 | 2,828,185 | 71.3×70.1×97.5 |

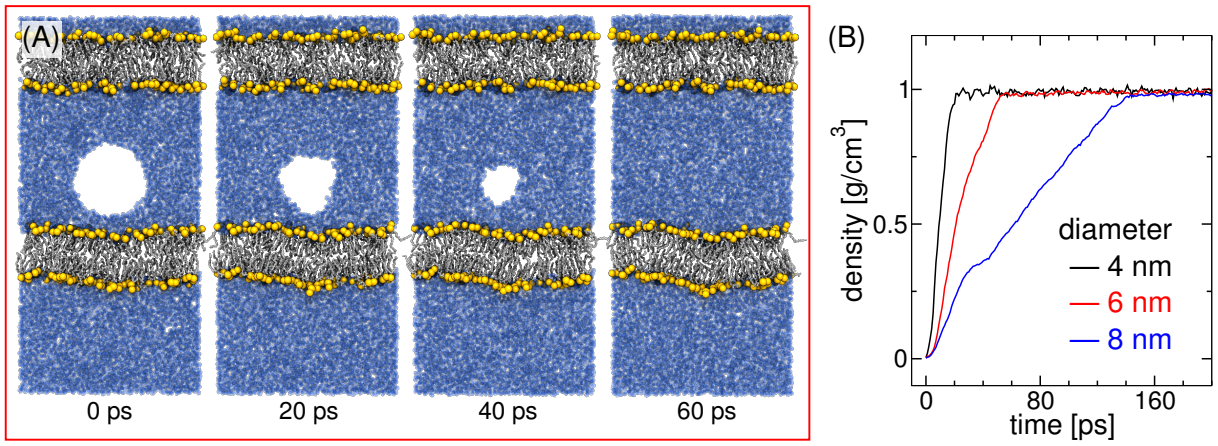


Figure S2: Molecular dynamics simulations of bubble collapse. **(A)** Cross-section of the simulation system at different times after the release of the restraints maintaining the bubble. A restraint is applied to the center of mass of the lower membrane, permitting the force exerted on it to be measured. The purpose of the upper membrane is to dissipate the upward traveling disturbance created by the collapsing bubble, thereby preventing it from reaching the lower membrane as conservation of energy and momentum would dictate. To accomplish this, a Langevin thermostat is applied to the upper membrane only. The initial diameter of the bubble in this example is 6 nm. Water molecules are represented as transparent blue spheres. Lipids are shown as gray tubes with phosphate and choline moieties highlighted as yellow spheres. **(B)** The mass density of the spherical region initially forming the bubble as a function of time after the geometrical restraints are released. The results are shown for bubbles of three different initial diameters. The limiting value approaches the density of bulk model water.

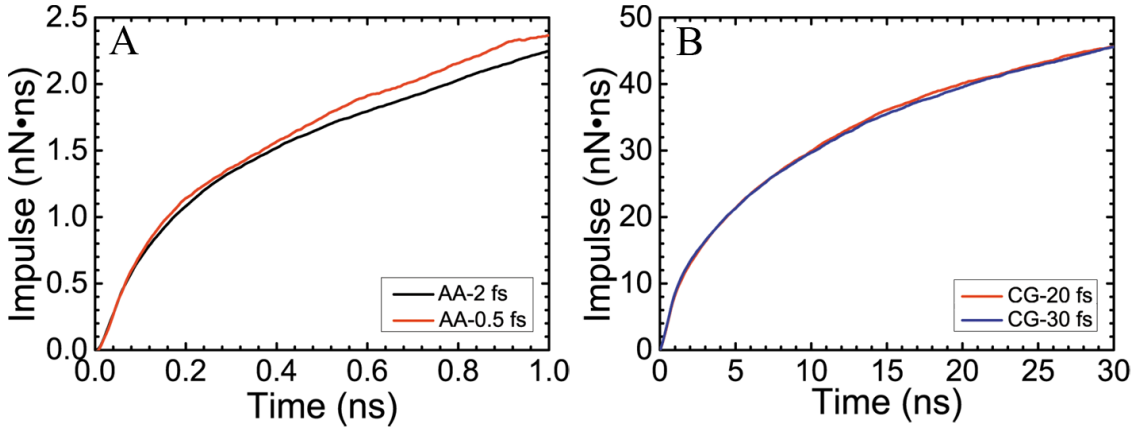


Figure S3: Effect of the time step on the impulses delivered to the membrane during collapse of a cavitation bubble. **(A)** Atomistic model, and **(B)** coarse-grained model. The diameter of the bubbles is 6 and 20 nm for the atomistic and the coarse-grained simulations, respectively. As shown, the impulses on the membrane obtained with the different models are nearly identical for the corresponding systems, which suggests that the atomistic simulations with a 2 fs time step and the coarse-grained simulations with a 30 fs time step are suitable to characterize the collapse of cavitation nanobubbles.

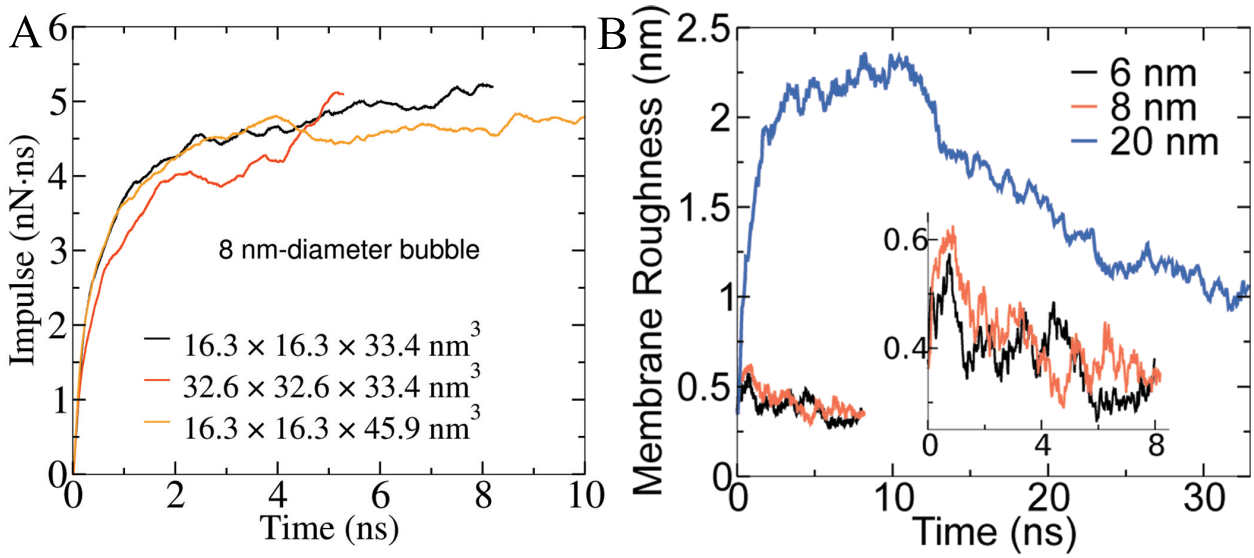


Figure S4: **(A)** Impulse on the membrane for the collapse of a 8 nm-diameter bubble for systems of different sizes. **(B)** Root-mean-square roughness of the membrane surface nearest the bubble as a function of time. **(Inset)** Magnification of the roughness for the 6– and 8 nm-diameter bubbles.

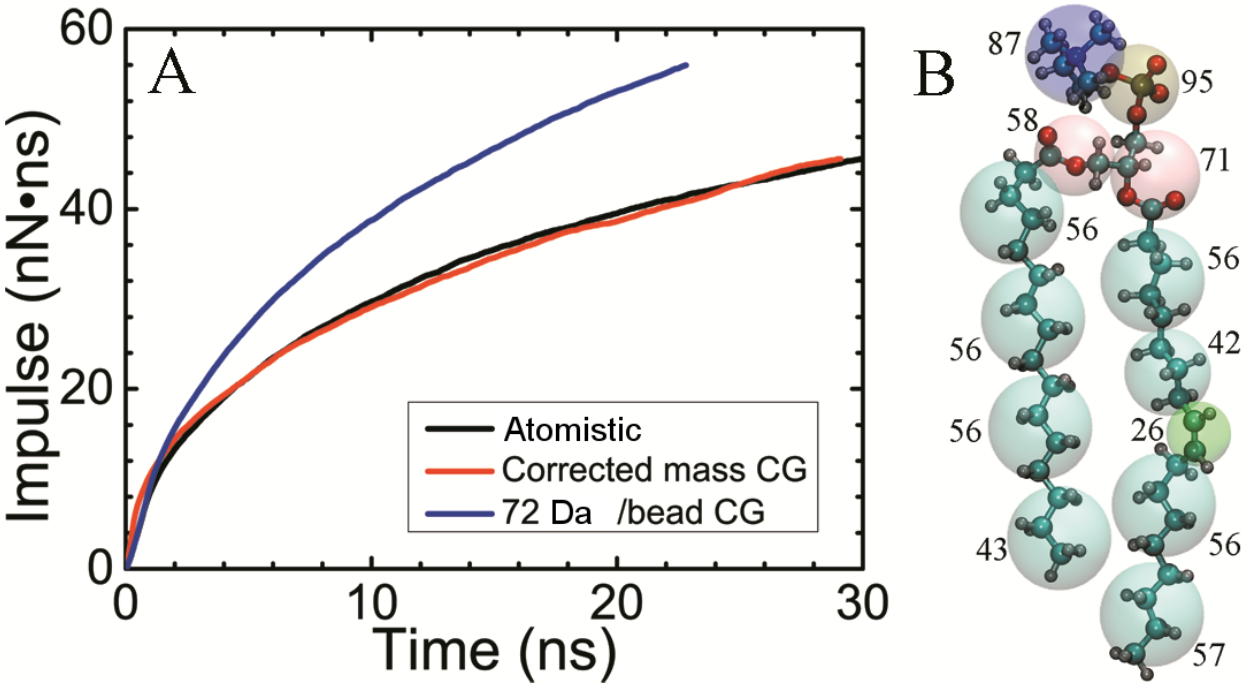


Figure S5: **(A)** Comparison of the impulse on the membrane during collapse of a 20 nm-diameter bubble in coarse-grained simulations using MARTINI standard bead masses (72 Da) or correct bead masses and atomistic simulations. **(B)** Coarse-grained mapping strategy for a POPC molecule.

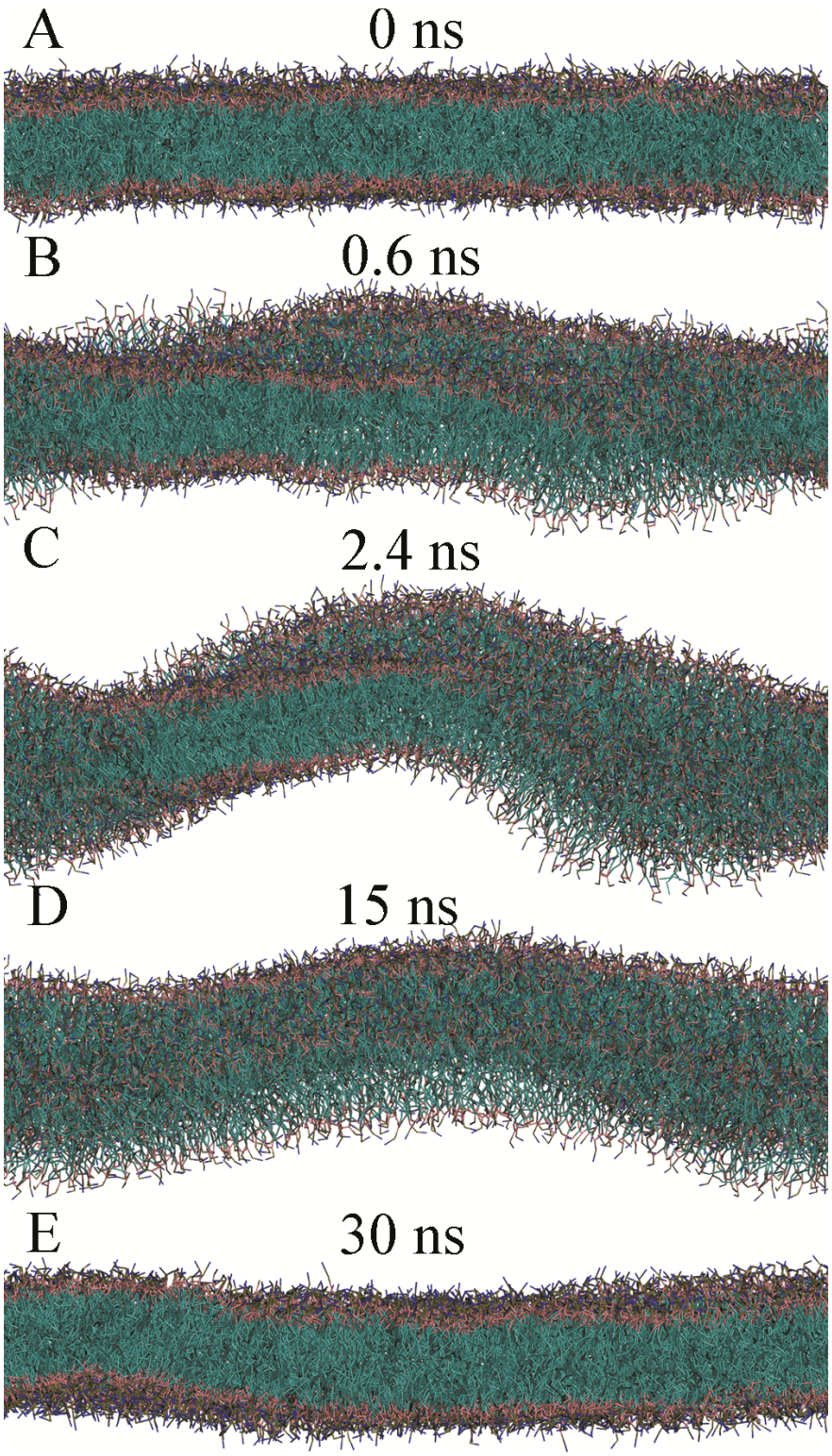


Figure S6: Deformation of a POPC membrane due to the collapse of a 20 nm-diameter bubble. The membrane was pulled by strong upward forces in the initial stage of the collapse, leading to the appearance of a positive peak around 2.4 ns, and then recovered in tens of nanoseconds.

# Calculation of impulse per unit area

Stringent assumption: All the effect of the collapse is concentrated in a certain surface area, A, on the membrane (Figure S7 (left)).

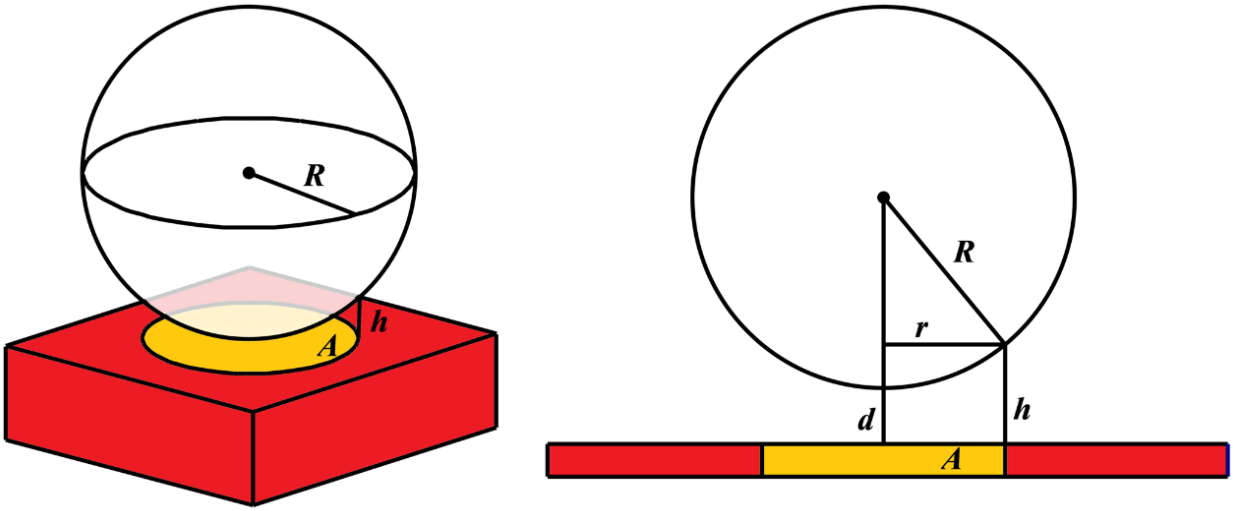


Figure S7: Three-dimensional (left) and two-dimensional (right) schematic representation of the collapse of a bubble at the surface of the membrane. $d$ is the minimum distance between the surface of the bubble and the membrane in the simulations. Here, $d = 2$ nm. We assume that the impulse in negligible if the distance between the surface of the bubble and the membrane is larger than a threshold, $h$. Here $h$ is set to 8 nm. It ought to be noted, however, that changes of $h$ of several nanometers (e.g. $6 \leq h \leq 10$ nm ) do not affect the order of magnitude of the result.

The stressed area is

$$A = \pi r^2$$

Because

$$\begin{aligned} r &= \sqrt{R^2 - [R - (h - d)]^2} \\ &= \sqrt{2R(h - d) - (h - d)^2}, \end{aligned}$$

then

$$I_A = I_{\text{total}}/A = \frac{cD^{2.15}}{\pi(h-d)[2R-(h-d)]} = \frac{c_0 D^{2.15}}{D-(h-d)}.$$

When $h = 8$ nm, $h - d = 6$ nm, and $c_0 = 0.0033$.

For bubbles used in experiments, the diameters often reach tens of micrometers, thus $D \gg h - d$. Then,

$$I_A = c_0 D^{1.15}.$$

For 10 $\mu$m-diameter bubbles,

$$I_A = 0.0033 \times 10000^{1.15} = 131 \text{ Pa} \cdot \text{s}.$$

For 100 $\mu$m-diameter bubbles,

$$I_A = 0.0033 \times 100000^{1.15} = 1856 \text{ Pa} \cdot \text{s}.$$

## References


(1) Basconi, J. E.; Shirts, M. R. Effects of Temperature Control Algorithms on Transport Properties and Kinetics in Molecular Dynamics Simulations. *J. Chem. Theory Comput.* **2013**, *9*, 2887–2899.

(2) Lugli, F.; Höfinger, S.; Zerbetto, F. The Collapse of Nanobubbles in Water. *J. Am. Chem. Soc.* **2005**, *127*, 8020–8021.

(3) Phillips, J. C.; Braun, R.; Wang, W.; Gumbart, J.; Tajkhorshid, E.; Villa, E.; Chipot, C.; Skeel, R. D.; Kale, L.; Schulten, K. Scalable Molecular Dynamics with NAMD. *J. Comput. Chem.* **2005**, *26*, 1781–1802.

(4) Klauda, J.; Venable, R.; Freites, J.; O'Connor, J.; Tobias, D.; Mondragon-Ramirez, C.; Vorobyov, I.; MacKerell Jr, A.; Pastor, R. Update of the CHARMM All-Atom Additive Force Field for Lipids: Validation on Six Lipid Types. *J. Phys. Chem. B* **2010**, *114*, 7830–7843.

(5) Hénin, J.; Shinoda, W.; Klein, M. United-atom Acyl Chains for CHARMM Phospholipids. *J. Phys. Chem. B* **2008**, *112*, 7008–7015.

(6) Darden, T. A.; York, D. M.; Pedersen, L. G. Particle Mesh Ewald: An $N \log N$ Method for Ewald Sums in Large Systems. *J. Chem. Phys.* **1993**, *98*, 10089–10092.

(7) Comer, J.; Schulten, K.; Chipot, C. Calculation of Lipid-Bilayer Permeabilities Using an Average Force. *J. Chem. Theory Comput.* **2014**, *10*, 554–564.

(8) Tuckerman, M. E.; Berne, B. J.; Martyna, G. J. Reversible Multiple Time Scale Molecular Dynamics. *J. Phys. Chem. B* **1992**, *97*, 1990–2001.

(9) Miyamoto, S.; Kollman, P. A. SETTLE: An Analytical Version of the SHAKE and RATTLE Algorithm for Rigid Water Molecules. *J. Comput. Chem.* **1992**, *13*, 952–962.

(10) Andersen, H. Rattle: A "velocity" Version of the Shake Algorithm for Molecular Dynamics Calculations. *J. Comp. Phys.* **1983**, *52*, 24–34.

(11) Marrink, S.; Risselada, H.; Yefimov, S.; Tieleman, D.; De Vries, A. The MARTINI Force Field: Coarse Grained Model for Biomolecular Simulations. *J. Phys. Chem. B* **2007**, *111*, 7812–7824.

(12) Feller, S. E.; Zhang, Y. H.; Pastor, R. W.; Brooks, B. R. Constant Pressure Molecular Dynamics Simulations — The Langevin Piston Method. *J. Chem. Phys.* **1995**, *103*, 4613–4621.

(13) Santo, K. P.; Berkowitz, M. L. Shock wave interaction with a phospholipid membrane: Coarse-grained computer simulations. *J. Chem. Phys.* **2014**, *140*, 054906.